Published in final edited form as:

Anal Chem. 2020 September 01; 92(17): 11681–11686. doi:10.1021/acs.analchem.0c01568.

Simultaneous Assessment of Intracellular and Extracellular pH using Hyperpolarized [1-^{13}C]Alanine Ethyl Ester

Jun Chen[1], **Edward P. Hackett**[1], **Jaspal Singh**[1], **Zoltán Kovács**[1], **Jae Mo Park**[1,2,3,*]

[1]Advanced Imaging Research Center, University of Texas Southwestern Medical Center, Dallas, TX 75390-8568

[2]Department of Radiology, University of Texas Southwestern Medical Center, Dallas, TX 75390-8568

[3]Department of Electrical and Computer Engineering, University of Texas at Dallas, Richardson, TX 75080

Abstract

Tissue pH is tightly regulated *in vivo*, being a sensitive physiological biomarker. Advent of dissolution dynamic nuclear polarization (DNP) and its translation to humans stimulated development of pH-sensitive agents. However, requirements of DNP probes such as biocompatibility, signal sensitivity, and spin-lattice relaxation time (T_1) complicate *in vivo* translation of the agents. Here, we developed a ^{13}C-labeled alanine derivative, [1-^{13}C]-L-alanine ethyl ester, as a viable DNP probe whose chemical shift is sensitive to the physiological pH range, and demonstrated the feasibility in phantoms and rat livers *in vivo*. Alanine ethyl ester readily crosses cell membrane while simultaneously assessing extracellular and intracellular pH *in vivo*. Following cell transport, [1-^{13}C]-L-alanine ethyl ester is instantaneously hydrolyzed to [1-^{13}C]-L-alanine, and subsequently metabolized to [1-^{13}C]lactate and [^{13}C]bicarbonate. The pH-insensitive alanine resonance was used as a reference.

Graphical Abstract

*Corresponding Author jaemo.park@utsouthwestern.edu.

Author Contributions

J.C., Z.K., and J.M.P. participated in the study design. J.C., E.P.H. and J.M.P. performed HP and MRI experiments. J.C., J.S., and Z.K. synthesized and verified the synthesis of alanine ethyl ester. All the authors contributed to data interpretation and manuscript writing.

Supporting Information.

General experimental and chemical synthetic methods, additional supporting figures (Figure S1. T_1 decay; Figure S2. pH-dependent chemical shift difference between alanine and alanine ethyl ester; Figure S3. alanine ethyl ester degradation in plasma), and a supporting table (Table S1. pH-dependence of chemical shifts of alanine and alanine ethyl ester).

The authors declare no competing financial interests.

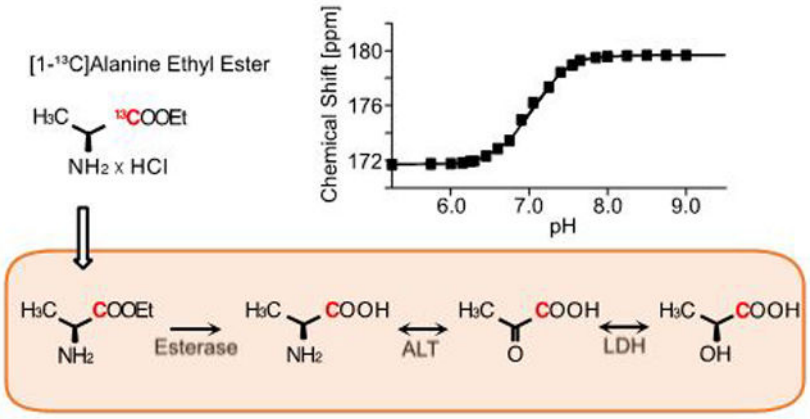

INTRODUCTION

Cellular pH is an important physiological parameter that is tightly regulated in living organisms by intrinsic buffer systems. Metabolic diseases, like inflammation, ischemia and numerous cancers, are accompanied with aberrant extracellular pH (pH_e).[1-3] Specifically, the metastatic development of many cancers is associated with acidic pH_e.[4-6] A significant decrease in pH_e was also correlated to immune responses in acute infection as well as chronic inflammatory diseases.[7] Intracellular pH (pH_i) is controlled within a narrower range, with homeostatic disruption implicated in both cell proliferation and cell death.[8] For instance, pH_i of cancer is low and gets lower towards the necrotic core[9,] and metabolic acid-base disorders occur alongside liver diseases.[10] Moreover, intracellular acidification has been observed in most types of apoptosis, autophagy and mitophagy.[8,11] Lysosomal acidification is a marker in aging and several neurodegenerative diseases.[12-14] Conversely, intracellular alkalinization is related to malignant transformation in cancer.[15,16] Thus, imaging modalities that can assess intracellular and extracellular pH *in vivo* are both highly valuable to investigate pathogenesis, assessment of disease progression, and monitor therapeutic responses.

Several imaging modalities have been proposed to assess pH non-invasively. Most pH probes were developed for sensing pH_e due to the diverse clinical relevance and the dynamic pH variation. In particular, magnetic resonance imaging (MRI) is the major approach for non-invasive pH imaging.[17-19] Dynamic nuclear polarization (DNP) of ^{13}C-labled substrate and its rapid dissolution process allowed *in vivo* ^{13}C MRI or MR spectroscopy (MRS)[20,21], providing opportunities to develop MR-based ^{13}C-labeled pH-sensitive sensors. The most well-studied pH probe is hyperpolarized (HP) [^{13}C]bicarbonate (HCO_3^-), which can detect pH by the peak ratios of $H^{13}CO_3^-/^{13}CO_2$.[22] However, utility of the technique is reserved by limited solubility of bicarbonate, low polarization level, short effective T_1, low signal to noise ratio (SNR) of CO_2, and lack of internal reference.[22,23] Other exogenous MR agents such as [^{13}C,^{15}N]N-(2-acetamido)-2-aminoethanesulfonic acid (ACES) and [1,5-$^{13}C_2$]zymonic acid (ZA) were proposed as pH-sensing probes, and the pH-dependent chemical shift changes were demonstrated *in vitro*.[24,25] However, ACES and ZA have very

short T_1 and require an internal chemical shift reference. Moreover, ZA is not very soluble in aqueous solution.

For measuring pH_i, the most common *in vivo* method applicable to humans is ^{31}P MRS, which measures the pH-sensitive chemical shift of intracellular inorganic phosphate (P_i) relative to pH-independent reference peaks such as phosphocreatine (PCr).[26] However, it is difficult to resolve P_i resonance from other peaks such as phosphodiesters or phosphomonoesters in the ^{31}P spectra[27], and internal frequency references are overlapped by other metabolites in certain tissues (e.g., PCr in tumors).[28] Moreover, imaging P_i and reference peak is impractical due to the inherently short T2. A recent study demonstrated feasibility of measuring cytosolic pH using ^{13}C chemical shifts of HP organic phosphates such as glyceronephosphate and 3-phosphoglycerate.[29] This is potentially achievable using carbohydrate as HP substrates, but even [U-^{2}H, U-^{13}C]glucose, one of the most promising candidates, has a T_1 value of less than 10 s.[30] Due to technical difficulties in developing pH_i-specific probes, essentially no alternative exogenous probe was developed to measure pH_i *in vivo*. Therefore, practical non-invasive imaging methods for *in vivo* pH_e and pH_i need to be established.

Generally, HP ^{13}C-probes with pH-dependent chemical shifts are more reliable in pH measurement than those with pH-derived peak ratios because quantifying chemical shift differences are more accurate and less prone to signal sensitivity. Amino acids and derivatives have excellent potential of being a pH biosensor with pH-determined chemical shifts.[31] Amino acids can be chemically modified to be sensitive to physiological pH range and the T_1 values are favorable when ^{13}C is labeled in the carboxylic group. In addition, their membrane permeable derivatives, such as ethyl ester, may accelerate the cellular uptake and allow for concurrent investigation of pH_i, pH_e, and amino acid metabolism *in vivo*.

Alanine is the principal amino acid released by skeletal muscle and taken up by the liver. Previous studies showed that HP [1-^{13}C]-L-alanine has a long T_1 at 3 T and can be used to monitor hepatic redox states under different nutrient condition through [1-^{13}C]lactate-to-[1-^{13}C]pyruvate ratio.[32,33] However, amount of the intracellular products from [1-^{13}C]-L-alanine was limited by the activity of alanine-serine-cysteine transporter (ASCT).[34] In this study, we developed HP [1-^{13}C]-L-alanine ethyl ester as a novel pH sensor for MRI and demonstrated the performance both *in vitro* and *in vivo*. It is very membrane permeable with a broad change in chemical shift in physiological pH range. The rapid cellular transport allows detection of pH_e and pH_i simultaneously as well as investigation of alanine metabolism with improved sensitivity.

EXPERIMENTAL SECTION

[1-^{13}C]-L-alanine ethyl ester was synthesized by esterification of commercially available [1-^{13}C]-L-alanine (Sigma Aldrich, St. Louis, MO). For analysis of the pH dependency, ^{13}C NMR spectra were acquired on a 9.4-T NMR spectrometer (Varian medical systems, Palo Alto, CA, USA). Chemical shifts of 500-μL of 10-mM [1-^{13}C]-L-alanine ethyl ester or [1-^{13}C]-L-alanine in aqueous solution at different pH titrated with NaOH were measured with t-butanol as reference for chemical shift.

A GE SPINlab™ polarizer, which operates at 0.8 K in a 5-T magnet, was used for DNP of [1-^{13}C]-L-alanine and [1-^{13}C]-L-alanine ethyl ester. Both *in vitro* polarization measurements and *in vivo* animal MRS were performed at a clinical 3-T MR scanner (GE Discovery 750w). [1-^{13}C]-L-alanine samples were prepared as described previously.[33] 6.2M of [1-^{13}C]alanine ethyl ester was prepared in 3:1 w/w water:glycerol with 15-mM OX063. The dissolved sample was adjusted to pH 7.5 with 500 μL of 250-mM Tris-HCl buffer. The liquid-state polarization levels and T_1 of the HP substrates were estimated using a ^{1}H/^{13}C dual-tuned birdcage radiofrequency (RF) coil (Ø = 80 mm) and a pulse-and-acquire sequence.

pH-sensing capability of [1-^{13}C]-L-alanine ethyl ester was evaluated using Eppendorf tubes, containing 200-μL of Tris-HCl buffer at pH 6.5, 7.0 and 7.5, respectively. HP [1-^{13}C]-L-alanine ethyl ester was inserted into the tubes and mixed with the buffer solutions prior to placing at the center of the rat coil. A single timepoint two-dimensional free induction decay (FID) chemical shift imaging (CSI) was acquired.

For the *in vivo* studies, healthy male Wistar rats (n = 7) were used. A custom-built ^{13}C surface coil (single loop, Ø = 28 mm) was placed on top of the liver area for both RF excitation and data acquisition. 80-mM HP [1-^{13}C] alanine or [1-^{13}C] alanine ethyl ester was injected intravenously as a bolus (1 mmol/kg body weight, up to 4.0 mL, injection rate = 0.25 mL/s), immediately followed by a dynamic ^{13}C MRS scan (FID CSI, 10° hard pulse RF excitation, repetition time = 3 s, scan time = 4 min).

The amount of metabolic products (e.g., alanine ethyl ester, alanine, lactate) from HP alanine or alanine ethyl ester was quantified by integrating the corresponding peaks in the time-averaged spectra then normalizing to the total ^{13}C signal (tC), which was the sum of all the time-averaged ^{13}C peaks. The results were reported as mean ± standard error. For evaluating statistical significance, a paired t-test was used to compare HP alanine and HP alanine ethyl ester results. The detailed experimental procedures are available in the Supporting Information.

RESULTS AND DISCUSSION

The synthesis and the chemical shift of [1-^{13}C]-L-alanine ethyl ester was confirmed by ^{13}C NMR at 9.4 T. A representative ^{13}C MR spectrum of a mixture of [1-^{13}C]-L-alanine ethyl ester and [1-^{13}C]-L-alanine showed [1-^{13}C]-L-alanine ethyl ester peak at 172.3 ppm and [1-^{13}C]-L-alanine peak at 176.3 ppm (Figure 1A) in pH 7.0. Liquid-state polarization of [1-^{13}C]-L-alanine ethyl ester was estimated as 22.5 %, which is ~85,600x signal enhancement of the thermal polarization at 3 T. T_1 of [1-^{13}C]-L-alanine ethyl ester was measured as 49.0 s (Figure 1B, Figure S1). T_1 of [1-^{13}C]-L-alanine could be also measured from alanine residual (1–2 %) in the sample (63.9 s), which was similar to the literature.[33]

Thermal NMR scans at 9.4 T showed that the chemical shift of [1-^{13}C]-L-alanine ethyl ester increased with pH (Figure 2A, Table S1). The chemical shift was stable from pH 4.5 (171.7 ppm) to 6.5 (171.9 ppm), and quickly increased to 179.5 ppm at pH 10. The pK_a was 8 at 175.69 ppm. The chemical shift of [1-^{13}C]-L-alanine stayed stable from pH 4.5 to 7.8 (176.6

ppm), then increased to 186 ppm at pH 13 with a pK_a at 10, which agreed with previous publication.[31] The pH-dependent chemical shift difference between [1-^{13}C]-L-alanine and [1-^{13}C]-L-alanine ehtyl ester is shown in Figure S2. The phantom imaging study using three cylindrical vials that contained HP [1-^{13}C]-L-alanine ethyl ester solutions with pH of 6.5, 7.0, and 7.5 confirmed that the chemical shift of [1-^{13}C]-L-alanine ethyl ester was pH-dependent near the physiologically relevant pH range (Figure 2). The pH-derived chemical shift changes in the HP phantom study were consistent with the thermal measurement at 9.4 T.

In vivo performance of HP [1-^{13}C]-L-alanine ethyl ester was evaluated in rat liver, and compared with HP [1-^{13}C]-L-alanine. Figure 3 shows time-averaged ^{13}C spectra from a representative rat liver, acquired with an injection of HP [1-^{13}C]-L-alanine or [1-^{13}C]-L-alanine ethyl ester. Significantly larger [1-^{13}C]lactate (184.0 ppm) peak (66.7 ± 13.5 % increase) was detected from HP [1-^{13}C]-L-alanine ethyl ester (lactate/total carbon [tC] = 0.0091 ± 0.0045, $p < 0.05$) than that of HP [1-^{13}C]-L-alanine (lactate/tC = 0.0054 ± 0.0026, n = 3). [1-^{13}C]pyruvate (173.0 ppm) production could not be detected as the peak was overlapped with [1-^{13}C]-L-alanine ethyl ester peak (172 ppm). [^{13}C]Bicarbonate ($H^{13}CO_3^-$) was measured as (HCO_3^-/tC = 0.0006 ± 0.0001 from alanine, and 0.0008 ± 0.0005 from alanine ethyl ester, $p = 0.36$), but detection was not reliable due to the limited signal sensitivity and susceptible to the nutritional state and the size of the animals. L-alanine ethyl ester was rapidly hydrolyzed into alanine *in vivo*, generating a large peak of [1-^{13}C]-L-alanine. A separate experiment using fresh rat blood serum showed that the contribution of blood esterase in converting [1-^{13}C]-L-alanine ethyl ester to [1-^{13}C]-L-alanine is negligible (Figure S3). Sum of the cellular products (lactate, bicarbonate, alanine) from HP [1-^{13}C]-L-alanine ethyl ester relative to the total carbon (tC) was higher (products/tC = 0.366 ± 0.032) than the products (lactate, bicarbonate) from HP [1-^{13}C]-L-alanine (products/tC = 0.007 ± 0.002, $p = 0.003$), suggesting that alanine ethyl ester uptake was significantly larger than alanine uptake.

From the [1-^{13}C]-L-alanine ethyl ester, two [1-^{13}C]-L-alanine ethyl ester peaks – peak ***e*** (173.5 ppm) and peak ***i*** (172.2 ppm) were detected in rat liver (Figure 4). The peak ***i*** accumulated and diminished one step ahead of the product [1-^{13}C]-L-alanine. While the peak ***e*** matched the chemical shift of [1-^{13}C]-L-alanine ethyl ester at pH 7.4 for hepatic extracellular pH, the peak ***i*** matched the chemical shift at pH 7.0 for intracellular pH.[35] The *in vivo* behavior of intracellular and extracellular HP [1-^{13}C]-L-alanine ethyl ester and its conversion to [1-^{13}C]-L-alanine could be further characterized using the time-resolved ^{13}C MRS in rat liver. The rapid buildup and clearance of the peak ***e*** suggests that it represents extracellular [1-^{13}C]-L-alanine ethyl ester. Conversely, the peak ***i*** indicates its identity of intracellular [1-^{13}C]-L-alanine ethyl ester. The subsequent alanine appearance indicates intracellular conversion of alanine ethyl ester. However, the contribution of blood esterase to the alanine conversion is limited as the activity of rat plasma esterase is much lower than the dose given[36,] and thus, not able to hydrolyze the large amount of alanine ethyl ester within the HP-detectable time window as we demonstrated in rat blood (Figure S1). On the other hand, intracellular esterase activity is significantly higher than plasma level in rodents.[37] Therefore, *in vivo* imaging of rat liver using HP [1-^{13}C]-L-alanine ethyl ester can detect

intracellular alanine as well as distinguishing intracellular alanine ethyl ester from the extracellular alanine ethyl ester.

HP [1-^{13}C]-L-alanine ethyl ester outperforms other pH-sensing HP probes in multiple aspects. First, T_1 of [1-^{13}C]-L-alanine ethyl ester is outstanding (49 s) as compared to other pH probes: 31–35 s for [^{13}C]bicarbonate (3 T), 23 s for [^{13}C, ^{15}N]ACES (3 T), and 17 s for [1,5-^{13}C]ZA (7 T).[22,24,25,38] Second, [1-^{13}C]-L-alanine ethyl ester is more soluble and the polarization level is higher than [^{13}C]bicarbonate and [1,5-^{13}C]ZA. Third, [1-^{13}C]-L-alanine ethyl ester determines pH from the chemical shift displacements, which are insensitive to the peak SNR or *in vivo* T_1, whereas ratio-determined pH-mapping methods require both peaks to be in high SNRs and additional information such as *in vivo* T_1 relaxation of the peaks for reliable pH analysis. Moreover, the amount of chemical shift dispersion of [1-^{13}C]-L-alanine ethyl ester in the physiologically relevant pH range (6.4–7.7) is large (3 ppm, ~95 Hz at 3 T). For an *in vivo* pH-sensing probe, the ideal pK_a would be ~7.5. Other alanine derivatives can be considered for improved pK_a. Lastly, HP [1-^{13}C]-L-alanine ethyl ester provides an internal reference peak, [1-^{13}C]-L-alanine, as the chemical shift of [1-^{13}C]-L-alanine is stable in physiological pH between 6.0 and 8.0, ranging from 176.62 to 176.76 ppm (Figure 2A, Table S1), while other HP probes such as [^{13}C]bicarbonate, [^{13}C,^{15}N]ACES and [1,5-^{13}C]ZA require additional reference.

Previous studies of HP [1-^{13}C]-L-alanine demonstrated its utility to investigate hepatic alanine metabolism.[32,33] In particular, [1-^{13}C]lactate and [1-^{13}C]pyruvate produced from HP [1-^{13}C]-L-alanine in liver are primarily from intracellular hepatic metabolism, allowing *in vivo* assessment of intracellular redox-state (NADH/NAD^+) from the ratio of [1-^{13}C]lactate to [1-^{13}C]pyruvate.[33] The efficacy of HP [1-^{13}C]-L-alanine to assess cellular redox state is dependent on the function of ASCTs. However, intracellular concentration of [1-^{13}C]-L-alanine is limited by the activity of ASCT2, and as a result, the amount of intracellular products is miniscule.[34] As alanine ethyl ester is a lipophilic analog of alanine that bypasses the ASCTs, its transport across the cell membrane is nearly instantaneous while alanine transporter ASCT2 depends on sodium ions, energy, and pH.[39,40] Thus, as compared to alanine, alanine ethyl ester can be transported into the cell, hydrolyzed, and metabolized into lactate, pyruvate and bicarbonate more efficiently despite the shorter T_1. However, [1-^{13}C]-L-alanine ethyl ester overlaps with [1-^{13}C]pyruvate, therefore, cannot be used to assess the redox state. Moreover, potential toxicity of [1-^{13}C]-L-alanine ethyl ester needs to be tested. Alternative strategies include co-injection of HP [2-^{13}C]-L-alanine and [1-^{13}C]-L-alanine ethyl ester and may develop an ultimate imaging tool for comprehensive assessment of *in vivo* cellular microenvironment by providing pH_i, pH_e, intracellular redox, and alanine metabolism.

HP [1-^{13}C]-L-alanine ethyl ester has several potential immediate applications. For instance, extracellular pH is decreased in many cancers and the altered pH_e is related to cancer cell motility and aggressiveness.[6] In addition, spatiotemporal pH heterogeneity in cancer correlates with therapeutic resistance and tumor progression with respect to maintaining stemness, differentiation capability, and extracellular matrix remodeling.[41] Moreover, pH for human cerebral cells are maintained at 7.0– 7.2, and lactic acidosis leads to irreversible

damage in ischemic tissue.[2] Thus, non-invasive imaging of pH would be helpful for prognosis and diagnosis of malignant tissues and ischemic tissues.

CONCLUSION

In conclusion, we developed [1-^{13}C]alanine ethyl ester as a cell-permeable HP substrate that can be metabolized *in vivo* to assess both pH_i and pH_e and to explore cellular alanine metabolism. The proposed design approach of esterification of pH-sensitive HP substrate can be applicable to develop other versatile HP probes for sensing extracellular and intracellular microenvironment as well as assessing metabolic utilization of the substrates simultaneously.

Supplementary Material

Refer to Web version on PubMed Central for supplementary material.

ACKNOWLEDGMENT

This work was supported by The Welch Foundation (I-2009-20190330 to J.M.P.); UT Dallas Collaborative Biomedical Research Award (UTD 1907789 to J.M.P.); The Texas Institute for Brain Injury and Repair (to J.M.P.); The Mobility Foundation (to. J.M.P.); National Institutes of Health of the United States (P41 EB015908 to Z.K.).

REFERENCES

(1). Tannahill GM; O'Neill LAJ The emerging role of metabolic regulation in the functioning of Toll-like receptors and the NOD-like receptor Nlrp3. FEBS Lett. 2011, 585 (11), 1568–1572. [PubMed: 21565193]

(2). Rehncrona S; Rosén I; Siesjö BK Brain lactic acidosis and ischemic cell damage: 1. Biochemistry and neurophysiology. J Cereb Blood Flow Metab 1981, 1 (3), 297–311. [PubMed: 7328145]

(3). Rajamäki K; Nordström T; Nurmi K; Åkerman KEO; Kovanen PT; Öörni K; Eklund KK Extracellular acidosis is a novel danger signal alerting innate immunity via the NLRP3 inflammasome. J. Biol. Chem 2013, 288 (19), 13410–13419. [PubMed: 23530046]

(4). Griffiths L; Dachs GU; Bicknell R; Harris AL; Stratford IJ The influence of oxygen tension and pH on the expression of platelet-derived endothelial cell growth factor/thymidine phosphorylase in human breast tumor cells grown in vitro and in vivo. Cancer Res. 1997, 57 (4), 570–572. [PubMed: 9044826]

(5). Kato Y; Ozawa S; Tsukuda M; Kubota E; Miyazaki K; St-Pierre Y; Hata R-I Acidic extracellular pH increases calcium influx-triggered phospholipase D activity along with acidic sphingomyelinase activation to induce matrix metalloproteinase-9 expression in mouse metastatic melanoma. FEBS J. 2007, 274 (12), 3171–3183. [PubMed: 17540003]

(6). Estrella V; Chen T; Lloyd M; Wojtkowiak J; Cornnell HH; Ibrahim-Hashim A; Bailey K; Balagurunathan Y; Rothberg JM; Sloane BF; Johnson J; Gatenby RA; Gillies RJ Acidity generated by the tumor microenvironment drives local invasion. Cancer Res. 2013, 73 (5), 1524–1535. [PubMed: 23288510]

(7). Casimir GJ; Lefèvre N; Corazza F; Duchateau J; Chamekh M The Acid-Base Balance and Gender in Inflammation: A Mini-Review. Front Immunol 2018, 9, 475. [PubMed: 29593728]

(8). Lagadic-Gossmann D; Huc L; Lecureur V Alterations of intracellular pH homeostasis in apoptosis: origins and roles. Cell Death Differ. 2004, 11 (9), 953–961. [PubMed: 15195071]

(9). Swietach P; Vaughan-Jones RD; Harris AL; Hulikova A The chemistry, physiology and pathology of pH in cancer. Philos. Trans. R. Soc. Lond., B, Biol. Sci 2014, 369 (1638), 20130099. [PubMed: 24493747]

(10). Scheiner B; Lindner G; Reiberger T; Schneeweiss B; Trauner M; Zauner C; Funk G-C Acid-base disorders in liver disease. J. Hepa-tol 2017, 67 (5), 1062–1073.

(11). Yu L; Chen Y; Tooze SA Autophagy pathway: Cellular and molecular mechanisms. Autophagy 2018, 14 (2), 207–215. [PubMed: 28933638]

(12). Dehay B; Martinez-Vicente M; Caldwell GA; Caldwell KA; Yue Z; Cookson MR; Klein C; Vila M; Bezard E Lysosomal impairment in Parkinson's disease. Mov. Disord 2013, 28 (6), 725–732. [PubMed: 23580333]

(13). Nixon RA; Yang D-S Autophagy failure in Alzheimer's disease--locating the primary defect. Neurobiol. Dis 2011, 43 (1), 38–45. [PubMed: 21296668]

(14). Götzl JK; Mori K; Damme M; Fellerer K; Tahirovic S; Kleinberger G; Janssens J; van der Zee J; Lang CM; Kremmer E; Mar-tin J-J; Engelborghs S; Kretzschmar HA; Arzberger T; Van Broeckhoven C; Haass C; Capell A Common pathobiochemical hallmarks of progranulin-associated frontotemporal lobar degeneration and neuronal ceroid lipofuscinosis. Acta Neuropathol. 2014, 127 (6), 845–860. [PubMed: 24619111]

(15). Gillies RJ; Martinez-Zaguilan R; Peterson EP; Perona R Role of Intracellular pH in Mammalian Cell Proliferation. CPB 1992, 2 (3-4), 159–179.

(16). Reshkin SJ; Bellizzi A; Caldeira S; Albarani V; Malanchi I; Poignee M; Alunni-Fabbroni M; Casavola V; Tommasino M Na+/H+ exchanger-dependent intracellular alkalinization is an early event in malignant transformation and plays an essential role in the development of subsequent transformation-associated phenotypes. FASEB J. 2000, 14 (14), 2185–2197. [PubMed: 11053239]

(17). van Sluis R; Bhujwalla ZM; Raghunand N; Ballesteros P; Alvarez J; Cerdán S; Galons JP; Gillies RJ In vivo imaging of extracellular pH using 1H MRSI. Magn Reson Med 1999, 41 (4), 743–750. [PubMed: 10332850]

(18). Ward KM; Balaban RS Determination of pH using water protons and chemical exchange dependent saturation transfer (CEST). Magn Reson Med 2000, 44 (5), 799–802. [PubMed: 11064415]

(19). Gillies RJ; Raghunand N; Garcia-Martin ML; Gatenby RA pH imaging. A review of pH measurement methods and applications in cancers. IEEE Eng Med Biol Mag 2004, 23 (5), 57–64.

(20). Ardenkjaer-Larsen JH; Fridlund B; Gram A; Hansson G; Hansson L; Lerche MH; Servin R; Thaning M; Golman K Increase in signal-to-noise ratio of > 10,000 times in liquid-state NMR. Proc. Natl. Acad. Sci. U.S.A 2003, 100 (18), 10158–10163. [PubMed: 12930897]

(21). Golman K; Zandt RI; Lerche M; Pehrson R; Ardenkjaer-Larsen JH Metabolic imaging by hyperpolarized 13C magnetic resonance imaging for in vivo tumor diagnosis. Cancer Res. 2006, 66 (22), 10855–10860. [PubMed: 17108122]

(22). Gallagher FA; Kettunen MI; Day SE; Hu D-E; Ardenkjaer-Larsen JH; Zandt RI '.; Jensen PR; Karlsson M; Golman K; Lerche MH; Brindle KM Magnetic resonance imaging of pH in vivo using hyperpolarized 13C-labelled bicarbonate. Nature 2008, 453 (7197), 940–943. [PubMed: 18509335]

(23). Ghosh RK; Kadlecek SJ; Pourfathi M; Rizi RR Efficient production of hyperpolarized bicarbonate by chemical reaction on a DNP precursor to measure pH. Magn Reson Med 2014.

(24). Flavell RR; Morze Von C; Blecha JE; Korenchan DE; Van Criekinge M; Sriram R; Gordon JW; Chen H-Y; Subramaniam S; Bok RA; Wang ZJ; Vigneron DB; Larson PE; Kurhanewicz J; Wilson DM Application of Good's buffers to pH imaging using hyperpolarized (13)C MRI. Chem. Commun. (Camb.) 2015, 51 (74), 14119–14122. [PubMed: 26257040]

(25). Düwel S; Hundshammer C; Gersch M; Feuerecker B; Steiger K; Buck A; Walch A; Haase A; Glaser SJ; Schwaiger M; Schilling F Imaging of pH in vivo using hyperpolarized (13)C-labelled zymonic acid. Nat Commun 2017, 8, 15126. [PubMed: 28492229]

(26). Griffiths JR; Stevens AN; Iles RA; Gordon RE; Shaw D 31P-NMR investigation of solid tumours in the living rat. Biosci. Rep 1981, 1 (4), 319–325. [PubMed: 7295895]

(27). Ren J; Sherry AD; Malloy CR (31)P-MRS of healthy human brain: ATP synthesis, metabolite concentrations, pH, and T1 relaxation times. NMR Biomed 2015, 28 (11), 1455–1462. [PubMed: 26404723]

(28). Rata M; Giles SL; deSouza NM; Leach MO; Payne GS Comparison of three reference methods for the measurement of intracellular pH using 31P MRS in healthy volunteers and patients with lymphoma. NMR Biomed 2014, 27 (2), 158–162. [PubMed: 24738141]

(29). Jensen PR; Meier S Hyperpolarised organic phosphates as NMR reporters of compartmental pH. Chem. Commun. (Camb.) 2016, 52 (11), 2288–2291. [PubMed: 26725378]

(30). Rodrigues TB; Serrao EM; Kennedy BWC; Hu D-E; Kettunen MI; Brindle KM Magnetic resonance imaging of tumor glycolysis using hyperpolarized 13C-labeled glucose. Nat. Med 2014, 20 (1), 93–97. [PubMed: 24317119]

(31). Hundshammer C; Düwel S; Ruseckas D; Topping G; Dzien P; Müller C; Feuerecker B; Hövener JB; Haase A; Schwaiger M; Glaser SJ; Schilling F Hyperpolarized Amino Acid Derivatives as Multivalent Magnetic Resonance pH Sensor Molecules. Sensors (Basel) 2018, 18 (2), 600.

(32). Hu S; Zhu M; Yoshihara HAI; Wilson DM; Keshari KR; Shin P; Reed G; Morze, Von C; Bok R; Larson PEZ; Kurhanewicz J; Vigneron DB In vivo measurement of normal rat intracellular pyruvate and lactate levels after injection of hyperpolarized [1-(13)C]alanine. Magn Reson Imaging 2011, 29 (8), 1035–1040. [PubMed: 21855243]

(33). Park JM; Khemtong C; Liu S-C; Hurd RE; Spielman DM In vivo assessment of intracellular redox state in rat liver using hyperpolarized [1-(13) C]Alanine. Magn Reson Med 2017, 77 (5), 1741–1748. [PubMed: 28261868]

(34). Joseph SK; Bradford NM; McGivan JD Characteristics of the transport of alanine, serine and glutamine across the plasma membrane of isolated rat liver cells. Biochem. J 1978, 176 (3), 827–836. [PubMed: 747655]

(35). Lloyd MH; Iles RA; Simpson BR; Strunin JM; Layton JM; Cohen RD The effect of simulated metabolic acidosis on intracellular pH and lactate metabolism in the isolated perfused rat liver. Clin Sci Mol Med 1973, 45 (4), 543–549. [PubMed: 4751972]

(36). Rudakova EV; Boltneva NP; Makhaeva GF Comparative analysis of esterase activities of human, mouse, and rat blood. Bull. Exp. Biol. Med 2011, 152 (1), 73–75. [PubMed: 22803044]

(37). Bahar FG; Ohura K; Ogihara T; Imai T Species difference of esterase expression and hydrolase activity in plasma. J Pharm Sci 2012, 101 (10), 3979–3988. [PubMed: 22833171]

(38). Scholz DJ; Janich MA; Köllisch U; Schulte RF; Ardenkjaer-Larsen JH; Frank A; Haase A; Schwaiger M; Menzel MI Quantified pH imaging with hyperpolarized (13) C-bicarbonate. Magn Reson Med 2015, 73 (6), 2274–2282. [PubMed: 25046867]

(39). Oppedisano F; Pochini L; Galluccio M; Cavarelli M; Indiveri C Reconstitution into liposomes of the glutamine/amino acid transporter from renal cell plasma membrane: functional characterization, kinetics and activation by nucleotides. Biochim. Biophys. Acta 2004, 1667 (2), 122–131. [PubMed: 15581847]

(40). Chakrabarti AC Permeability of membranes to amino acids and modified amino acids: Mechanisms involved in translocation. Amino Acids 1994, 6 (3), 213–229.

(41). Korenchan DE; Flavell RR Spatiotemporal pH Heterogeneity as a Promoter of Cancer Progression and Therapeutic Resistance. Cancers (Basel) 2019, 11 (7), 1026.

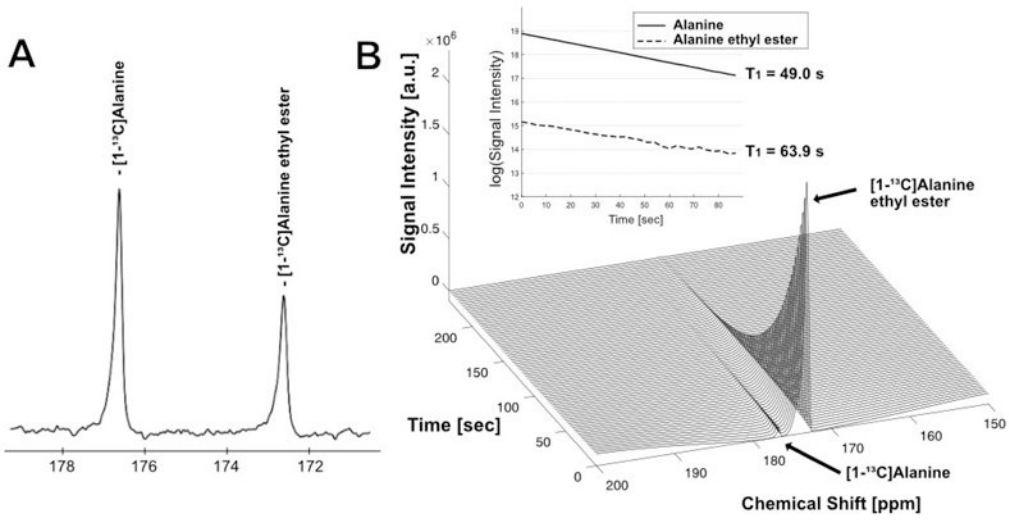

Figure 1.

NMR spectrum and T1 of alanine ethyl ester. (A) *In vitro* ^{13}C NMR spectrum (9.4 T) of a mixture of [1-^{13}C]-L-alanine and [1-^{13}C]-L-alanine ethyl ester. The peaks shown are [1-^{13}C]-L-alanine (176.3 ppm) and [1-^{13}C]-L-alanine ethyl ester (172.3 ppm). (B) Dynamic changes of ^{13}C MR spectrum of HP [1-^{13}C]-L-alanine ethyl ester in liquid-state (3 T).

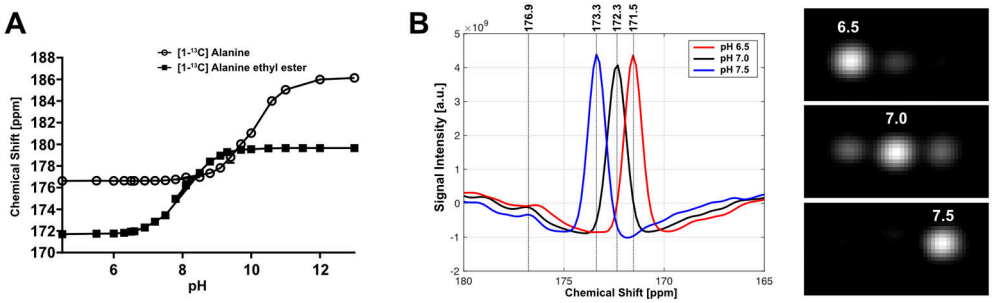

Figure 2.

pH-dependent chemical shift of [1-^{13}C]-L-alanine ethyl ester. (A) Chemical shifts of [1-^{13}C]-L-alanine and [1-^{13}C]-L-alanine ethyl ester in aqueous solution with pH ranging from 4.5 to 13.5 (9.4 T). (B) Spatially averaged MRS spectra (left) over phantoms of 80-mM HP [1-^{13}C]-L-alanine ethyl ester at pH 6.5 (red), pH 7.0 (black) and pH 7.5 (blue), respectively (3 T). Peak-integrated ^{13}C images (right) at central frequencies at 171.5, 172.3, and 173.3 ppm.

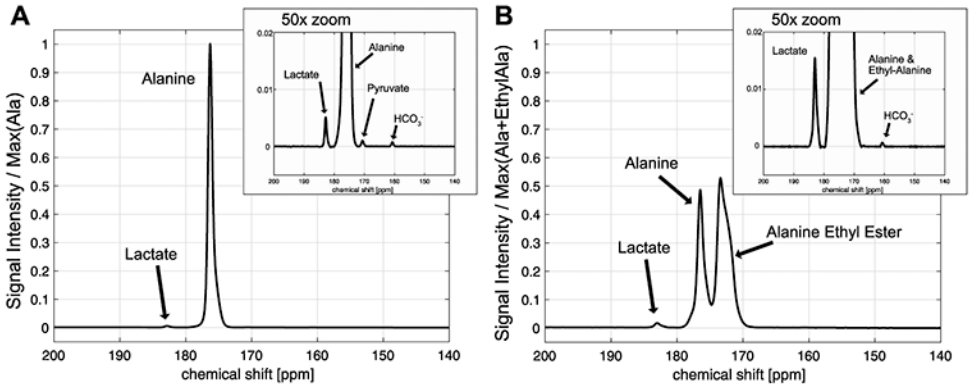

Figure 3.

Time-averaged ^{13}C signals from rat liver after injection of 80-mM HP [1-^{13}C]-L-alanine (A) or [1-^{13}C]-L-alanine ethyl ester (B). The spectrum from HP alanine is normalized to the [1-^{13}C]-L-alanine peak intensity and the [1-^{13}C]-L-alanine ethyl ester spectrum is normalized to sum of [1-^{13}C]-L-alanine and [1-^{13}C]-L-alanine ethyl ester peaks.

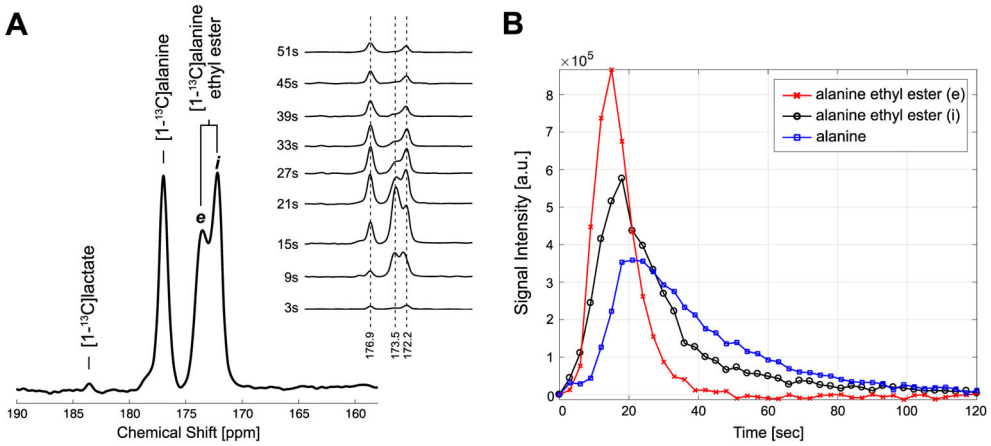

Figure 4.

In vivo spectrum of HP [1-^{13}C]-L-alanine ethyl ester and the products in rat liver. (A) Time-averaged and dynamic change of the spectrum acquired from rat liver after an injection of 80-mM HP [1-^{13}C]-L-alanine ethyl ester (3 T), (B) Time-courses of alanine and alanine ethyl ester obtained by integrating the peak values of the spectrum at each time point.